Broadband reflective cholesteric liquid crystalline gels: volume distribution of reflection properties and polymer network in relation with the geometry of the cell photopolymerization

Sabrina Relaix, Christian Bourgerette, Michel Mitov

Accepted version published in: *Liquid Crystals*, **34**, 1109-1018 (2007)

Broadband reflective cholesteric liquid crystalline gels: volume distribution of reflection properties and polymer network in relation with the geometry of the cell photopolymerization

Sabrina Relaix, Christian Bourgerette and Michel Mitov*

Centre d'Elaboration de Matériaux et d'Etudes Structurales (CEMES), CNRS,

Univ. Toulouse, BP 94347, 29 rue Jeanne-Marvig, F-31055 Toulouse cedex 4, France

The ultraviolet (UV) light absorbing properties of the liquid crystal (LC) constituent during the photo-induced elaboration of a cholesteric LC (CLC) gel may induce the broadening of the reflection bandwidth of the material, which situation is promoted by asymmetrical irradiation conditions (only one side of the cell is irradiated). The *in situ* structure of the polymer network, included in the LC, is investigated by transmission electron microscopy and the temperature-dependence of the reflection properties is examined; it is shown that the network has a structure gradient which is at the origin of the broadening phenomenon. The smallest reflection wavelength was shown like being located at the neighbouring of the cell side from which the UV light beam got into the material. *A priori*, this situation was unexpected since it is shown that this part of the gel is enriched with nematic (infinite-pitch CLC) network-forming material. This result is discussed in relation with the variation of the reflection band characteristics with the polymer concentration, which offers the opportunity to have an indirect access to the volume distribution of the cholesteric periodicities. For applications, broadband reflective cholesteric gels may be of interest for reflective polarizer-free displays or for the light management with smart electrically-switchable reflective windows.

Article history: Received 5 March 2007 / Accepted 4 July 2007

https://doi.org/10.1080/02678290701602876

* Corresponding author, email address: mitov@cemes.fr

1. Introduction

1.1. Property of selective light reflection by a cholesteric liquid crystal.

A selective light reflection is exhibited by a cholesteric liquid crystal (CLC) slab with a uniformly oriented Grandjean planar texture (*i.e.* the helix axis is perpendicular to the observation plane) [1, 2]. At normal incidence, the mean reflection wavelength λ_0 is related to the pitch p and the mean refraction index $\bar{n}$ by:

$$\lambda_0 = \bar{n}\, p.$$

$\bar{n}$ is the average of the ordinary (n_o) and extraordinary (n_e) refractive indices of the locally uniaxial structure: $\bar{n} = (n_o + n_e)/2$. The spectral width of the reflection band $\Delta\lambda$ is defined as:

$$\Delta\lambda = p\, \Delta n$$

where $\Delta n = n_e - n_o$ is the birefringence. Within $\Delta\lambda$, an incident unpolarized or linearly polarized light beam parallel to the helix axis is split into two opposite circularly polarized components, one of which is transmitted whereas the other is reflected. The sense of rotation of the latter one agrees with the helix screw sense. A wavelength out of $\Delta\lambda$ is simply transmitted. Compared to conventional pigmented color filters, a CLC slab has the special feature to combine several optical properties in one layer: it is not only a filter but also a reflector and a polarizer. Since Δn is limited to 0.3 – 0.4 for colorless organic compounds, $\Delta\lambda$ is limited to a few tens of nm in the visible spectrum, which means that CLC materials are effective for a certain color and not for the whole visible spectrum.

1.2. State of the art and objectives of the work

For switchable reflective devices, such as electro-optical glazing structures to be used for the dynamical controlling of the electromagnetic radiations, it is required to go beyond the usual limits of the reflection bandwidth of low molar mass CLCs. The choice of Polymer-Stabilized CLCs (PSCLCs) elaborated under specific ways has offered the opportunity to increase the reflection bandwidth [3-7]. Polymer-Stabilized Liquid Crystals (PSLCs) — also called Polymer Network-SLCs (PNSLCs) or LC gels — are formed by ultraviolet (UV) light polymerization of a small amount of bifunctional photoreactive monomers – typically between 3 and 10 wt.% – dissolved in a LC phase [8, 9]. The first standing result of forming a polymer network into the LC solvent is the transfer of the mesophase characteristics to the network morphology and structure during the *in situ* polymerization. As a consequence, several physical characteristics of the original structure, and consequently the texture, may be kept by the introduction of a large surface to volume ratio as compared to the usual orientation induced by the alignment properties of the cell surfaces. Several research groups have focused their attention on PSLCs due to the peculiar properties they present by comparison with low molar mass LCs ones. Depending on the pitch range, PSCLCs exhibit specific optical and electro-optical properties which give rise to bistable reflective displays or light shutters with normal-mode [10] and reversed-mode [11]. From the more recent literature related to PSCLCs, the following results have been reported: the effect of the UV light wavelength on polymer morphology and electro-optical properties of diffraction gratings [12], the reduction of the hysteresis loop of the reverse-mode PSCL cell by increasing the monomer concentration [13] and the use of PSCLCs for polarization-independent tunable-focus microlens arrays [14].

With the aim of increasing the reflection bandwidth of CLC structures, an earlier solution has consisted in the elaboration of a cholesteric layer with a pitch gradient. A UV light absorbing dye was used to create an intensity gradient of the UV light through the thickness of a solid CLC polymer network [15] or a switchable CLC gel [16]. Therefore, the polymerisation at the surface the closest to the UV light source is much faster than at the bottom of the layer. By blending a cholesteric diacrylate with a nematic (infinite-pitch cholesteric) monoacrylate, the former component has a twice as high probability as the nematic component to be incorporated in the polymer network [15]; at low intensity, depletion of the chiral compound near the top of the cell generates a pitch gradient through the thickness of the layer. As a complementary possibility for going beyond the usual limits of the reflection band of low molar mass CLCs, the increase of the reflected light intensity – never greater than 50% of ambient (unpolarized) light – may also be aimed, as recently demonstrated by using PSCLCs with a thermally-induced inversion of the helicity sense [17, 18]. The present work deals with the broadening of the reflection band of PSCLCs without the intervention of a foreigner UV light absorbing dye but like the consequence of the natural absorbing properties of the LC constituent of the gel. We will highlight this phenomenon by using three different sets of irradiation conditions and, more generally, we will show that it is possible to monitor the bandwidth amplitude by playing with the screening effect due to the LC component of the gel. This result was briefly reported by us in a previous letter intended for a broad readership [19]. The scope of the present paper is to give a detailed description of the bandwidth broadening property by presenting direct reflection profiles from one side of the cell to the other one in relation with the geometry of the cell photopolymerization (asymmetrical *vs.* symmetrical conditions, presence of a UV light filter) and transmission electron microscopy (TEM) investigations of the *in situ* polymer morphology. A peculiar attention is given to the unexpected situation which consists in having the smallest reflection

wavelength at the neighbouring of the cell side which is enriched in nematic network-forming liquid crystalline material.

2. Experimental Section

2.1. LC blend. A room-temperature CLC mixture (BL094 from Merck Ltd.) is mixed with bifunctional photoreactive nematic mesogens (RM257 from Merck Ltd.) at a concentration ratio of 91 wt.% of LC / 9 wt.% monomers, with a small amount of photonitiator Irgacure 907 (from Ciba-Geigy; 2 wt.% compared to the RM257 amount). The blend exhibits a cholesteric phase at room temperature. From texture investigations by polarized light microscopy, the isotropic phase appears at 75°C.

2.2. Cell characteristics. The blend is introduced at 83°C by capillarity in a 8 μm (±0.7 μm) thick ITO-coated glass cell (from EHC CO. Ltd.; type FF). In order to induce a planar alignment, the surfaces have been treated with rubbed polyimide (the plates were assembled with their rubbing directions making an angle of 180°C). Then the cell is quenched down from 70°C to the room temperature. When observed by polarized optical microscopy in transmittance mode, the cell exhibits a well aligned reflective Grandjean planar texture with a moderate presence of oily streaks.

2.3. UV light curing conditions. The cell was kept at room temperature and, for polymerization purposes, illuminated for 30 minutes with UV light centered at 365 nm and with a power equal to 0.1 mW/cm^2 as measured with a radiometer (UVR-365 from Prolabo). In the following, the as-called *asymmetrical conditions* correspond to an irradiation from one

single side (with a black substrate disposed under the cell) whereas the *symmetrical conditions* correspond to an irradiation from both sides and simultaneously.

2.4. Spectrophotometry. The transmission and reflection spectra were recorded by using the HR2000CG-UV-NI spectrophotometer (from Ocean Optics) associated to an optical microscope. When measurements in the infrared spectrum are required (cf. Figures 8 and 9), the UV-3100 spectrophotometer (from Shimadzu) is used for all the measurements. The incident light is unpolarized. All the baselines were recorded with air (a mirror) in the beam path for the transmittance (reflectance) measurements. The multiple secondary peaks present in the transmittance spectra correspond to the wave interference due to the internal reflection between the two inner surfaces of the cell substrates; the periodicity is related to the film thickness.

2.5. Preparation of materials for TEM and observation conditions. Resin is substitued for the LC component by immersing the gel cell in a bath of LR White Resin diluted in a solvent (methanol); the concentration of resin in solvent is progressively increased from one bath to the next one to optimize the filling of the network porosity. From such a *modus operandi* it is expected to preserve the spatial distribution of the network into the cell volume. Finally, the cell is opened at room temperature, the material which consists in the polymer network embedded in a resin lump is removed and embedded in a second (epoxy) resin in order to be manipulated. 80 nm thick slices of cross-sections of the sample are cut with an ultramicrotome (Reichert) at room temperature. The cuts are observed by using a Philips CM12 transmission electron microscope.

3. Results

3.1. Polymerization under asymmetrical conditions

Figure 1 shows the transmittance spectra of the cell before and after the photopolymerization. Before curing, $\Delta\lambda$, as measured at the half-width of the peak, is about 80 nm. After curing, the reflection bandwidth is approximately located at the same mean wavelength and has been significantly increased: $\Delta\lambda$ is now equal to about 220 nm.

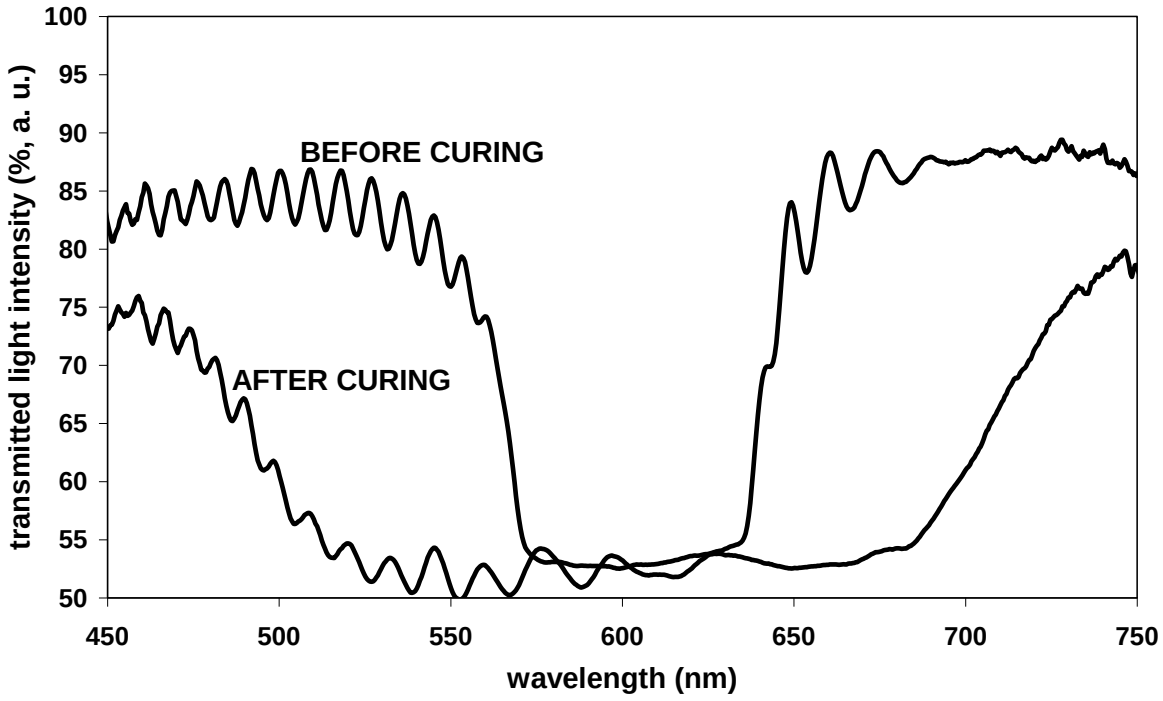

Figure 1. Transmitted light intensity as a function of wavelength before and after curing under asymmetrical conditions.

Figure 2 shows the reflection spectra of the cell after curing according to the side of the cell which is presented to the incoming light beam probe of the microscope–spectrophotometer. For analysis purposes, it is indeed relevant to make a discrimination between the side of the cell which was the nearest to the UV light source – as-called UP side

– and the other one, as-called DOWN side. Each reflection curve exhibits a main peak the position of which depends on the side.

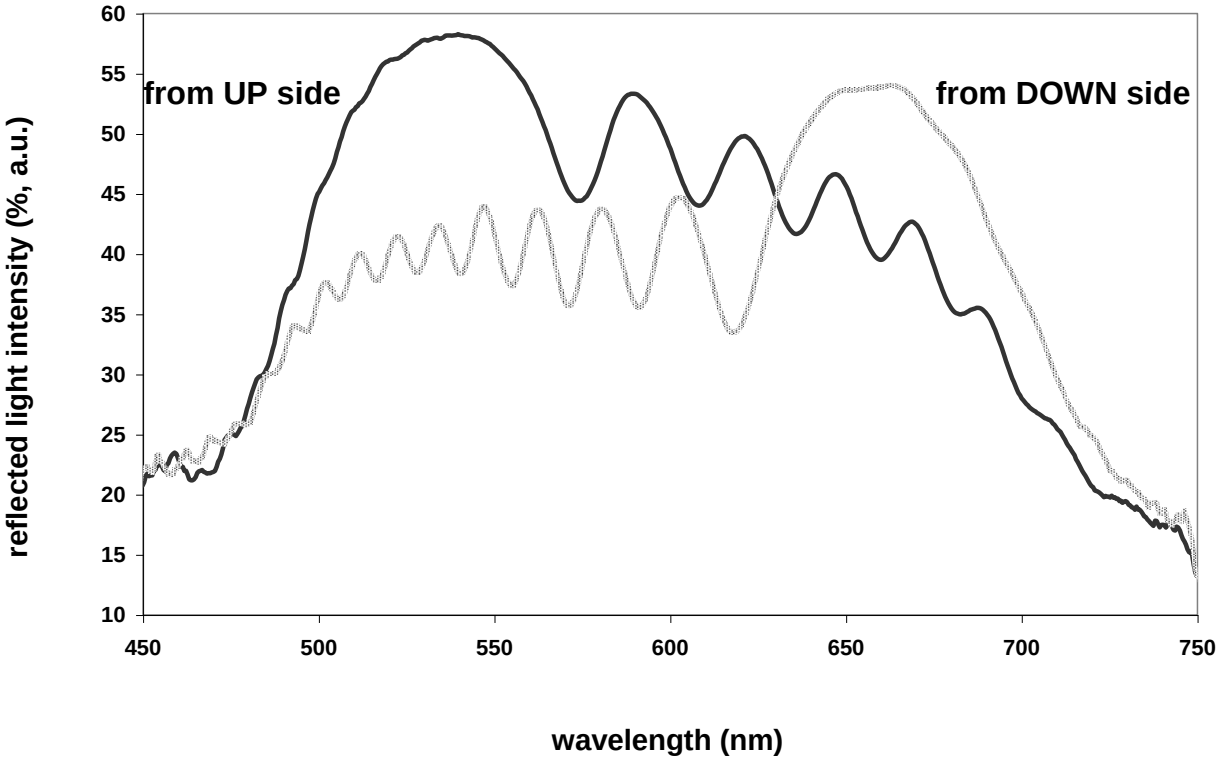

Figure 2. Reflected light intensity related to the UP and DOWN sides as a function of wavelength after curing under asymmetrical conditions.

The main peak is located at smaller (longer) wavelengths when the UP (DOWN) side is presented to the beam. The wavelength related to the main peak assigned to the UP (DOWN) side is about 540 nm (660 nm); when observed by polarized optical microscopy in reflection mode, the colour of the UP side is greenish whereas it is reddish for the DOWN side. Although the multiple secondary peaks correspond to the wave interference due to the internal reflection between the two inner surfaces of the cell substrates, it appears that color (Bragg) reflections with a weaker light intensity are also present at wavelengths between the positions of the two main peaks; the intensity is variable and lower in this part of the curves

due to a variable and non-optimum number of pitch lengths present in the material [20]. This first set of results suggests that the reflection properties are not monotonously distributed inside the volume of the gel – a situation from which a broadening of the reflection band may arise – and that the pitch of the hypothetical graded helical structure is longer close to the DOWN side than close to the UP one. The discussion will be focused on this key-result of the present publication.

In order to investigate a relation between the different reflection properties of the two sides, and the possible existence of a concentration gradient, we followed up the variation of the reflection spectra with the temperature. Figure 3 shows two sets of results depending on whether the UP or DOWN side of the cell is presented to the incoming light beam. The variation of the reflection wavelength with the temperature for the blend before curing is also reported for comparison purposes; in this case and like an evident fact, the reflection property stops at the clearing temperature (above 75°C).

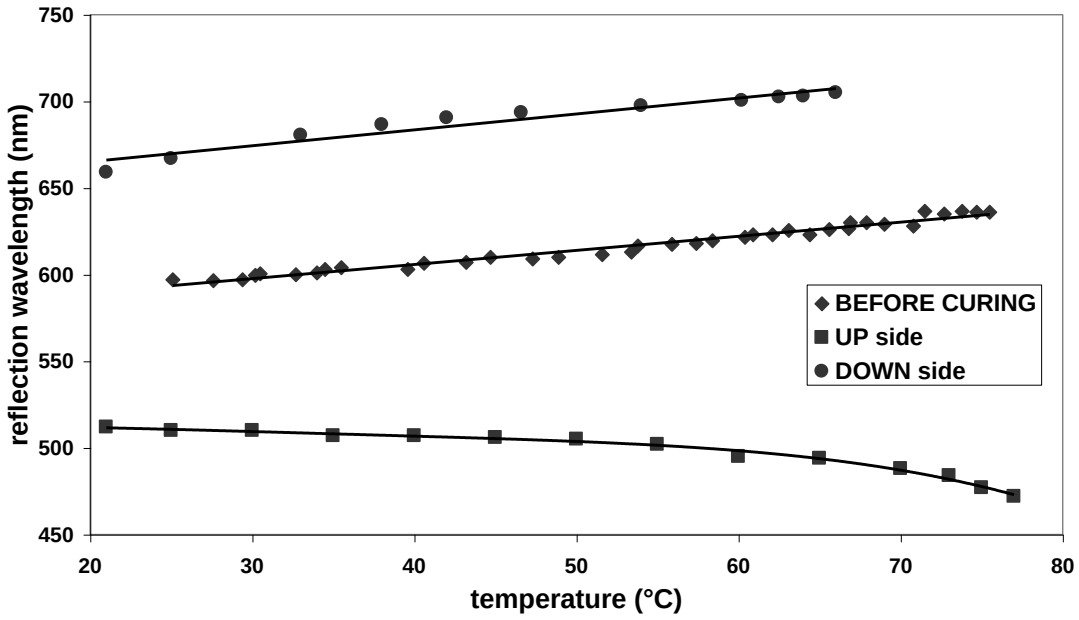

Figure 3. Reflection wavelength related to the UP and DOWN sides as a function of temperature after curing under asymmetrical conditions. The data related to the blend before curing are also reported.

A reflection wavelength assigned to the UP side is no more reported above 78°C because the measurements were uneasy due to the weak quantity of the related light intensity (and the limit of sensitivity of the spectrophotometer); however, it is important to notice that cholesteric planar textures may be observed by polarized optical microscopy (reflection mode) up to 150°C and above, like the consequence of the patterning effect of the polymer network located close to the UP side. PSLCs are indeed commonly described with a two-population model for the low molar mass LC [21]. One population – the free fraction – is weakly influenced by the presence of the polymer whereas the other one – the bound fraction – undergoes strong surface interactions with it. The bound fraction corresponds to LC molecules at the immediate surrounding of the polymer walls. The polymer morphology insures memory effects of the orientational order present when its formation occurs (anisotropic growth of polymer units, like oriented fibres as an example). Therefore, the regions of gel corresponding to the bound fraction will encompass the isotropic transition at a much more elevated temperature by comparison with the behavior of the free fraction, which has similarities with the behavior of the LC before its blending with the network-forming material. The report of a reflection wavelength assigned to the DOWN side also stops at 65°C due to the weak quantity of the related light intensity. When the temperature is increased from 20°C up to the clearing point, the wavelength is shifted towards slightly smaller (longer) values for the UP (DOWN) side.

On one hand, the variation of λ with the temperature for the blend and the DOWN side have similar behaviors. The DOWN side is mainly made of a free population of LC molecules (with a fraction of the network as oligomer chains at the very most), which situation could explain that the variation of λ is mainly dictated by the pitch variation. λ for the DOWN side is slightly but systematically located above the λ attached to the blend. This difference may be understood like the consequence of the composition of the CLC slab close

to the DOWN side which is different from the blend composition since it is deprived of a part of the network-forming material and includes a sparse network (oligomers) — like the TEM investigations will show it.

On the other hand, the variation corresponding to the UP side is quite different: the reflection wavelength slightly decreases with the temperature and close to the clarification temperature of the blend before curing. The UP side is made of a dense and thermally-stable network; the variation of the reflection wavelength would come from the (modest) variation of the mean optical index of the LC component (which decreases up to the isotropic point) included in the gel layer close to the UP side more than the pitch variation because the pitch is here locked in the network.

Thus, the results displayed in Figure 3 again suggest that the reflection wavelength is greater close to the DOWN side than close to the UP one and that the polymer concentration is larger close to the UP side.

3.2. Polymerization under symmetrical conditions

Since it is known that a broadening of the reflection band may arise from a UV light intensity gradient [15], we investigated the role of a dual-irradiation on the broadening property of the reflection bandwidth. We thus arranged a cell at half-distance between the two UV light sources. A mean power equal to 0.1 mW/cm^2 was measured on each plate of the sandwich-cell. In that case, the phenomenon of broadening of the reflection band is still present but less pronounced by comparison with the case of asymmetrical conditions: the reflection bandwidth is equal to about 160 nm *vs.* 220 nm in the former case, like we reported in [19]. The reflection spectra for both sides of the cell are displayed in Figure 4: the peaks are now very close and located around 620 nm.

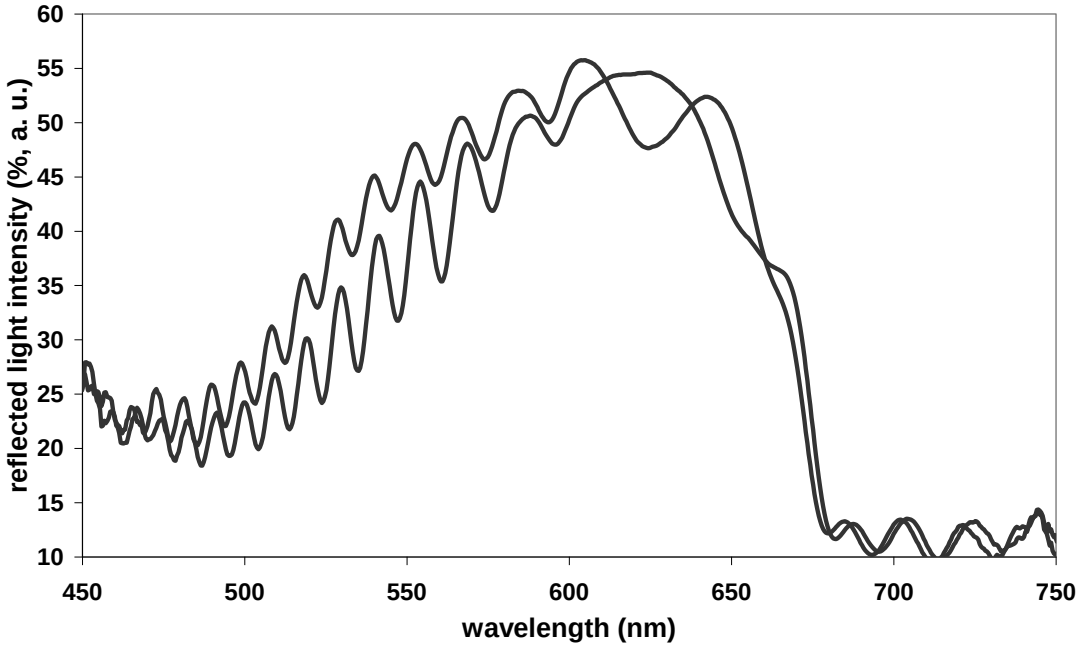

Figure 4. Reflected light intensity related to both sides of the cell as a function of wavelength after curing under symmetrical conditions.

The variations of the reflection wavelength with the temperature have now very close behaviors for both sides (Figure 5).

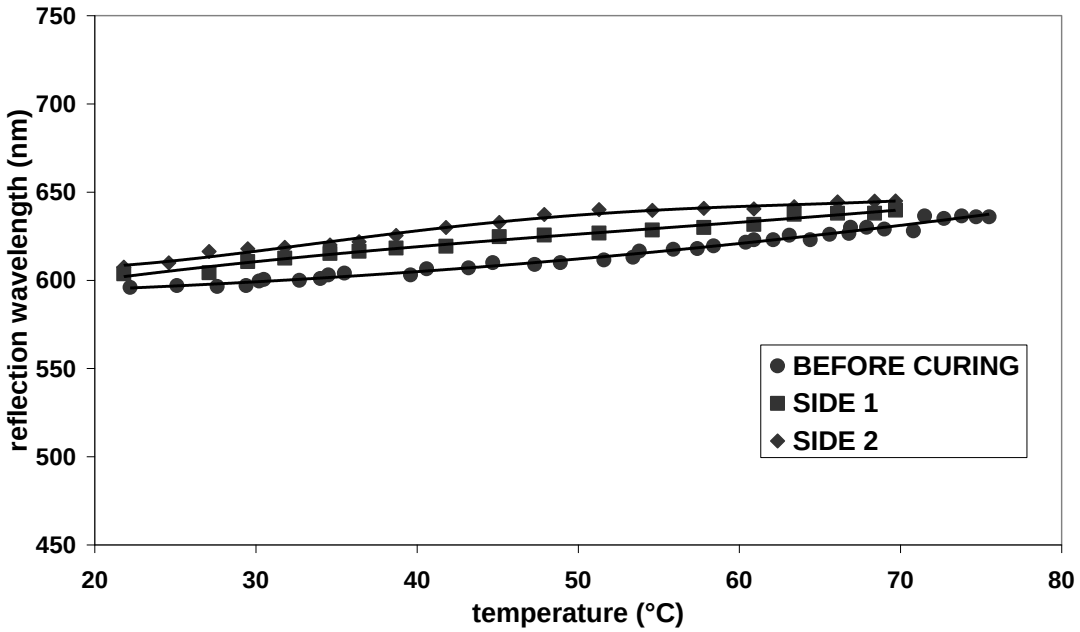

Figure 5. Reflection wavelength related to both sides of the cell as a function of temperature after curing under symmetrical conditions. The data related to the blend before curing are also reported.

They are located slightly above the curve assigned to the variation of the reflection wavelength before curing; however, the difference is very small and the relative position of curves, as well as their position with regard to the curve assigned to the blend, have no clear signification since the difference between values reported in Figure 5 are comprised in measurement errors. Thus, the asymmetry in the position of the reflection band is on the way to be lost in the case of a UV light irradiation from both sides and simultaneously. Under the hypothesis of a concentration gradient in polymer network at the origin of the pitch gradient, we can understand that this gradient will be modest, although still present, when the symmetry for the fabrication of the network in the LC volume is met. This result is evidenced by the proximity of curves in Figure 5 when we compare it to the dispersion of measurements in Figure 3. The fact that the reflection property of both sides is close to the one of the blend before curing shows that the quite homogeneous distribution of the cholesteric periodicity initially present in the CLC layer has been almost frozen in the gel structure and that the *in situ* formation of the polymer network has not a significant impact on the reflection property when the cell is irradiated on both sides and in the same time.

3.3. Polymerization under asymmetrical conditions in the presence of a UV light filter made with the LC component

Since the broadening of the reflection band might be related to a concentration gradient in the polymer morphology from the UP side of the cell to the DOWN one, a

progressive absorption of UV light by the LC constituent may be suspected. We then decided to cure the experimental cell when a cell filled with the pure LC (BL094) is attached to it (*i.e.*: the UP side). Such a geometry offers the opportunity to investigate the screening role of the LC constituent on the UV light beam and, in return, on the polymerization characteristics and the optical properties. The variation of the bandwidth with the thickness of the LC slab used like a filter was investigated; $\Delta\lambda$ linearly decreases when the thickness increases: whereas $\Delta\lambda$ is about 220 nm when the curing occurs without filter, it decreases from 180 to 100 nm when the filter thickness changes from 4 to 44 μm, like we reported in [19]. This result shows that the part of the UV light beam incoming on the experimental cell has been filtered by the LC cell and that the screening effect – from which a gradient network may arise – is strongly attenuated. Figure 6 gives a macroscopic evidence of this result by displaying a photograph of a large-size (2.6 x 5.2 cm) homemade cell filled with the blend when the curing occurs whereas a staircase-like filter-cell (Fig. 6.a) was attached to it.

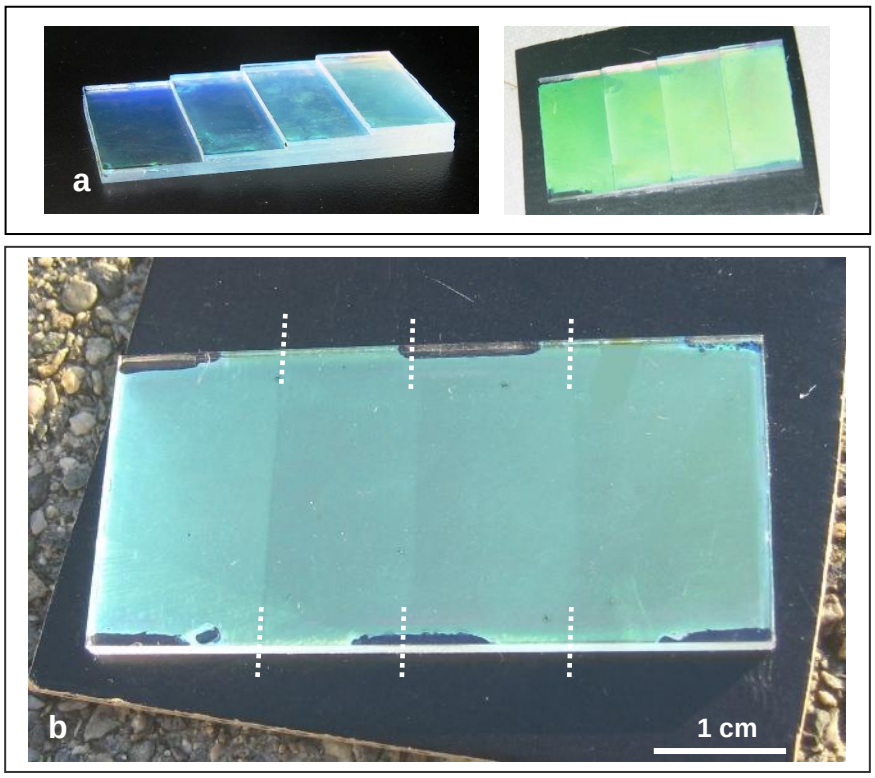

Figure 6. (a) The staircase-like filter: a thickness-gradient cell filled with BL094; lateral (left) and top (right) views are shown. (b) Large-size (2.6 x 5.2 cm) homemade cell after curing when the staircase-like filter was attached to one side during the UV light irradiation under asymmetrical conditions. The frontier zones corresponding to the interface between two successive steps of the filter (now removed) are visible; they are partially stressed with white dotted lines in the photograph.

In Figure 6.a: 1, 2, 3 and 4 LC slabs of BL094 are successively present from the left side of the filter to the right one; each LC slab is about 10 μm thick. A variation of the green reflection color can be observed in a direction parallel to the long side of the experimental cell (Fig. 6.b). The frontier zones, which are partially stressed with white dotted lines in Figure 6.b for presentation purposes, mark the limit between two successive steps of the staircase-like filter (which has been removed here).

3.4. Investigations of the polymer network distribution and morphology

TEM investigations definitively offer the valuable opportunity to bring information about the structure of the polymer network in relation with the UV light curing conditions. Figure 7 shows the micrographs of cross-sections of the polymer when the gel was fabricated under asymmetrical (Figure 7.a) or symmetrical (Figure 7.b) conditions. Figure 7.a clearly shows that the network is more concentrated close to the UP side of the cell. A scattered network is displayed at the neighbouring of the opposite side of the cell: this situation suggests that a discontinuous network, with oligomeric structures, is formed close to the DOWN side. Therefore a concentration-gradient network has been formed in the LC volume when the curing conditions are asymmetrical. Under the hypothesis of a concentration

gradient in polymer network at the origin of the pitch gradient, we can understand that this gradient is more modest when the symmetry conditions for the fabrication of the network in the LC volume are met and why a less broadened bandwidth is obtained in return. Indeed, Figure 7.b shows that the network morphology and distribution are qualitatively the same from one side to the other one by being symmetrical around the 'symmetry' axis as reported in the picture. Interestingly, it has to be noticed that a discrete concentration gradient is still present from each one of the surfaces. In both cases, a local orientation of chains of polymer beads may be distinguished in a direction parallel to the surfaces but this kind of organization does not appear to be dense and regular whereas we observed a periodic stratification reminiscent of the cholesteric fingerprint texture in 25 μm thick samples. These pictures are the first TEM visualization of the *in situ* distribution of a concentration-gradient polymer network in the volume of a PSLC.

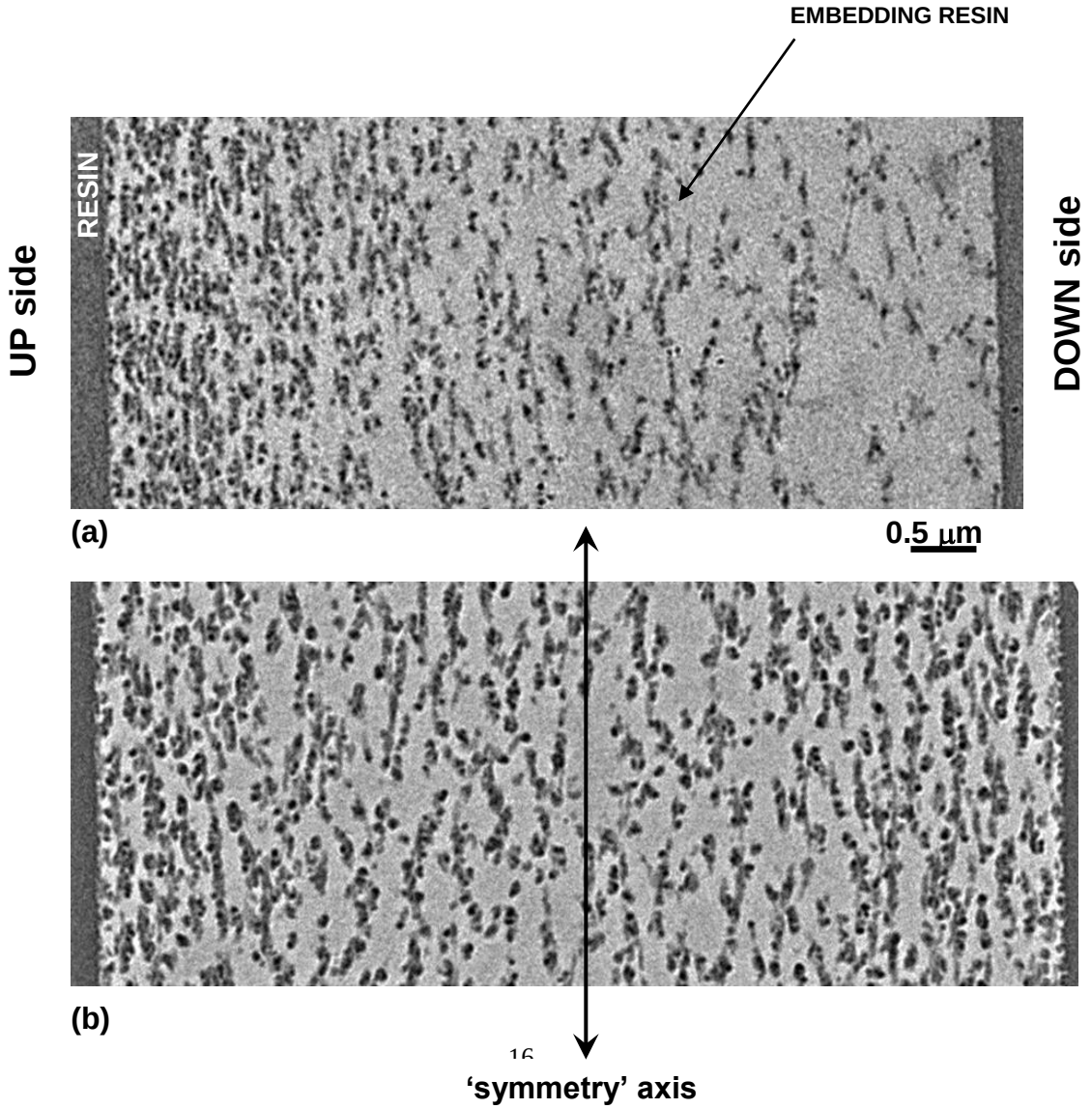

Figure 7. Transmission electron microscopy images of the polymer network embedded in a resin matrix, after dissolution of the LC, when the cell was irradiated: (a) from one side – the UP side (asymmetrical conditions) or: (b) simultaneously from both sides (symmetrical conditions).

4. Discussion

We have shown that a broadening of the reflection bandwidth in a PSCLC may arise from the formation a concentration-gradient polymer network, which is promoted by asymmetrical curing conditions as a consequence of the UV light screening made by the LC component. The polymer concentration is greater close to the UP side than close to the DOWN one. Consequently, since the network-forming material is a nematic LC (infinite-pitch CLC), the pitch would have been expected to be longer close to the UP side and like decreasing in a direction perpendicular to the UP substrate, as reported in literature [6, 22]. But this scenario is in apparent contradiction with the present reflection measurements, which correspond to the smallest reflection wavelength close to the UP side. We are going to discuss this point. Since the broadening of the reflection bandwidth comes from a network concentration which decreases from the UP to the DOWN side, it is relevant to investigate the variation of characteristics of the reflection band – λ and $\Delta\lambda$ – when the concentration in network-forming material varies.

Firstly, from Figure 8 (from transmittance measurements and under asymmetrical conditions) we learn that λ varies over a broad range from 540 up to 1800 nm, *i.e.* from the middle of the visible spectrum up to the infrared spectrum, when the RM257 concentration increases from a zero value (case of pure BL094) to 70 wt.%. It means that cholesteric periodicities with related λ well above the focused range of the present investigation (450–

750 nm) may be present in the helical structure of the gel layer. Besides, the position of the reflection band is here remarkably not affected by the polymerization process.

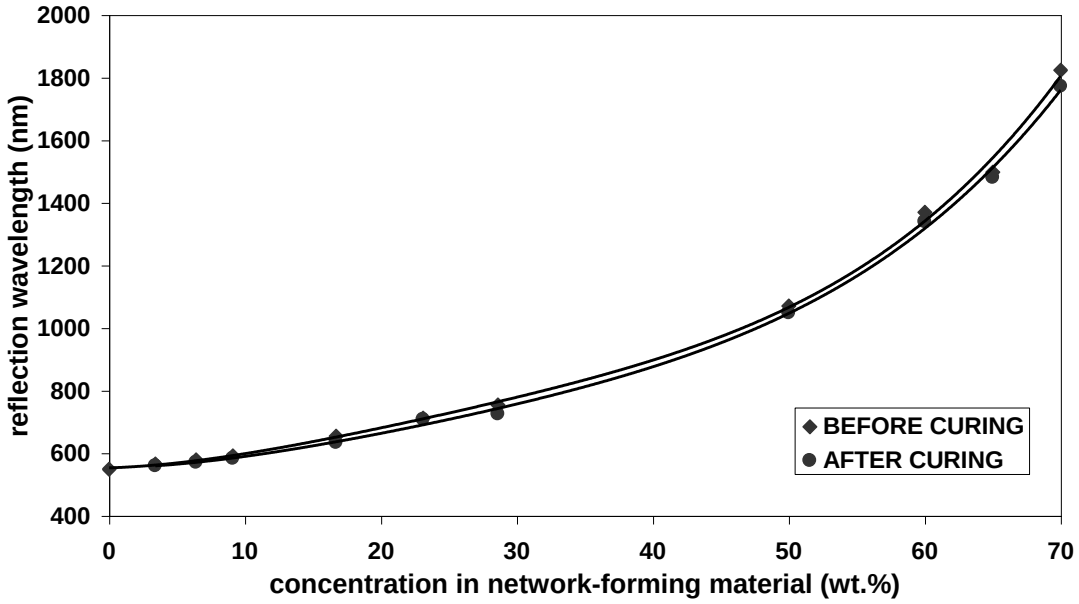

Figure 8. Reflection wavelength as a function of the concentration in network-forming material (RM257) before and after curing under asymmetrical conditions.

Secondly, the investigation of the variation of $\Delta\lambda$ with the RM257 concentration (from transmittance measurements and under asymmetrical conditions), in Figure 9, gives indirectly informations of paramount importance on the distribution of periodicities to be brought together with the polymer distribution as seen in Figure 7.a and suggests the following comments:

(i) The variation of $\Delta\lambda$ with the RM257 concentration exhibits a non-monotonous behavior. Especially, $\Delta\lambda$ increases in a quite broad range, from about 100 to 420 nm, when the RM257 concentration changes in a restricted range — from 4 to 17 wt.%.

(ii) Then, after an inflexion point, at about 20 wt.%, $\Delta\lambda$ decreases more slowly from 430 to 165 nm when the concentration varies from 23 to 60 wt.%.

(iii) Finally, $\Delta\lambda$ increases with a behavior similar to the blend one from 60 wt.%; the network concentration is so huge that a distinction between the free and bound fractions of LC molecules has no more sense and the material is constituted of LC molecules closely associated to the network (bound fraction). The fact that $\Delta\lambda$ is smaller after curing comes from a pitch decrease related to the volume shrinkage resulting from the reaction of polymerization and crosslinking; this behavior was also observed in the formation of CLC polymer networks [23] and CLC gels [18].

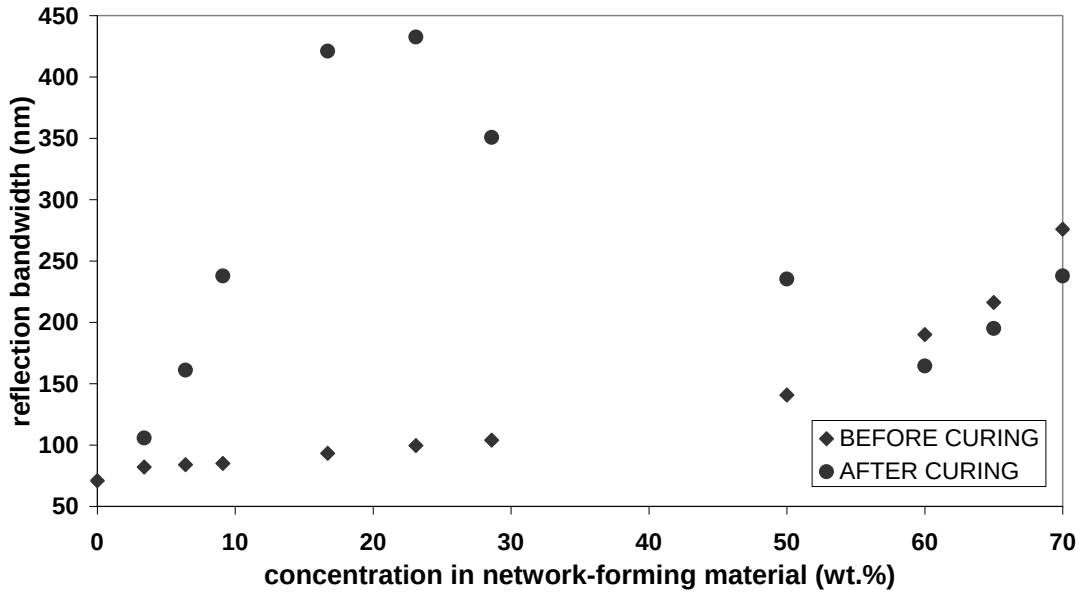

Figure 9. Reflection bandwidth as a function of the concentration in network-forming material (RM257) before and after curing under asymmetrical conditions.

Because the DOWN side is less enriched in polymer network, we could liken the composition of this region of the cell to the first part of the curve in Figure 9, *i.e.*: a region

for which a large set of reflection bandwidths is present and in relation with the smallest concentrations in network-forming material. It could explain why the reflection wavelength exhibited by the gel when the DOWN side is presented to the incoming beam is greater. As an example, and in comparison with what would happen at the surrounding of the UP side: it would be required to have a concentration profile sampled on 35 wt.% (from 25 to 60 wt.%), *vs*. 10 wt.% for the left part of curve in Figure 9 (from 7 to 17 wt.%), to reach a performance in common, *i.e.*: to have $\Delta\lambda$ which varies from 165 to 420 nm. In return, from Figure 8 it is shown that the reflection wavelength is out of the investigated range (> 750 nm) as soon as the concentration is more than about 28 wt.%; a 8 μm thick cell cannot offer the opportunity to let the helix to develop a sufficient number of turns at each range of pitch magnitude to give a reflection signal with a significant light flux amount [20]. Nevertheless, one or several periodicities sampled on all the range exhibited in Figure 9 are possible, with a distribution which includes the larger periodicities for the weakest concentrations in network-forming material, close to the DOWN side of the gel layer.

5. Conclusion

The natural UV light absorbing properties of the LC constituent during the photo-induced elaboration of a CLC gel may induce the broadening of the reflection bandwidth, which situation is promoted when only one side of the cell is irradiated. The polymer component was included in a resin by preserving its spatial distribution and the existence of a structure gradient, which is at the origin of the broadening phenomenon, was shown by TEM investigations of cross-sections. Direct reflection measurements have given clews on the distribution of the reflection wavelength inside the volume of the gel layer. The smallest reflection wavelength was shown like related to the neighbouring of the side close to

the UV light source when asymmetrical irradiation conditions are met. *A priori*, this situation was unexpected since the TEM investigations and the temperature-dependence of reflection properties have revealed that this side is enriched in nematic (infinite-pitch CLC) network-forming material. This result was discussed in relation with the variation of the characteristics of the reflection band with the polymer concentration which offers the opportunity to have an indirect access to the volume distribution of the cholesteric periodicities.

In view of practical applications, broadband reflective cholesteric gels may be of interest for reflective polarizer-free displays or for the light management for smart windows; the latter are electro-optical glazing structures, made with a cholesteric film sandwiched between glass panels, having reflective and transparent modes which are electrically-switchable.

Acknowledgements. We thank Ms. E. Nouvet for her help during the fabrication of LC cells.

References

[1] de Gennes, P.-G.; Prost, J. *The Physics of Liquid Crystals*; Oxford University Press: Oxford, 1993; pp. 264-268

[2] Kelker, H.; Hatz, R. *Handbook of Liquid Crystals*; Verlag Chemie: Weinheim, 1980; pp. 294-310.

[3] Leroux, N.; Fritz, W. J.; Doane, J. W.; L.-C. Chien. *Mol. Cryst. Liq. Cryst.* **1995**, *261*, 465.

[4] Li, J.-F.; Fan, B.; Li, L. *SID Symposium Digest* **1999**, *30*, 1066.

[5] Binet, C.; Mitov, M.; Mauzac, M. *J. Appl. Phys*. **2001**, *90*, 1730.

[6] Guillard, H.; Sixou, P. *Liq. Cryst.* **2001**, *28*, 933.

[7] Mitov, M.; Nouvet, E; Dessaud, N. *Eur. Phys. J. E* **2004**, *15*, 413.

[8] Crawford, G. P.; Zumer, S. eds. *Liquid Crystals in Complex Geometries*; Taylor and Francis: London, 1996.

[9] Dierking, I. *Adv. Mater*. **2000**, *12*, 167.

[10] Yang, D.-K.; L.-C. Chien, L.-C.; J. W. Doane. *Appl. Phys. Lett*. **1992**, *60*, 3102.

[11] West, J. L.; Akins, R. B.; Francl, J.; Doane, J. W. *Appl. Phys. Lett*. **1993**, *63*, 1471.

[12] Kang, S.-W.; Sprunt, S.; Chien, L.-C. *Chem. Mater*. **2006**, *18*, 4436.

[13] Huang, C. Y.; Ke S. W.; Chih, Y. S.; *Optics Comm*. **2006**, *266*, 198.

[14] Lin, Y.-H.; Ren, H.; Fan, Y.-H.; Wu, Y.-H.; Wu, S.-T. *J. of Appl. Phys*. **2005**, *98*, 043112.

[15] Broer, D.J.; Lub, J.; Mol, G.N. *Nature* **1995**, *378*, 467.

[16] Hikmet, R. A. M.; Kemperman, H. *Nature* **1998**, *392*, 476.

[17] Mitov , M.; Dessaud, N. *Nature Materials* **2006**, *5*, 361.

[18] Mitov, M.; Dessaud, N. *Liq. Cryst.* **2007**, *34*, 183.

[19] Relaix, S.; Bourgerette, C. ; Mitov, M. *Appl. Phys. Lett*. **2006**, *89*, 251907.

[20] We may consider than an helical structure with almost ten pitch lengths is required to come close to the maximum of reflected light intensity which is possible.

[21] Hikmet, R. A. M. *Mol. Cryst. Liq. Cryst*. **1991**, *198*, 357.

[22] Guillard, H.; Sixou, P.; Reboul, L.; Perichaud, A. *Polymer* **2001**, *42*, 9753.

[23] Broer, D. J.; Heynderickx, I. *Macromol*. **1990**, *23*, 2474.